EUROPEAN FUSION DEVELOPMENT AGREEMENT

EFDA–JET–CP(07)03/51

P.T. Lang, B. Alper, A. Boboc, R. Buttery, K.Gál, J. Hobirk, J. Neuhauser,
M. Stamp and JET EFDA contributors

ELM Triggering by Local Pellet Perturbations at JET

ELM Triggering by Local Pellet Perturbations at JET

P.T. Lang[1], B. Alper[2], A. Boboc[2], R. Buttery[2], K. Gál[3], J. Hobirk[1],
J. Neuhauser[1], M. Stamp[2] and JET EFDA contributors*

[1]*Max-Planck-Institut fnur Plasmaphysik, EURATOM Association, Boltzmannstr. 2, 85748 Garching, Germany*
[2]*EURATOM-UKAEA Fusion Association, Culham Science Centre, OX14 3DB, Abingdon, OXON, UK*
[3]*KFKI-RMKI, EURATOM Association, P.O. Box 49, H-1525 Budapest-114, Hungary*
** See annex of M.L. Watkins et al, "Overview of JET Results ",*
(Proc. 21st IAEA Fusion Energy Conference, Chengdu, China (2006)).

Preprint of Paper to be submitted for publication in Proceedings of the
34th EPS Conference on Plasma Physics,
(Warsaw, Poland 2nd - 6th July 2007)

1. AIM OF THE INVESTIGATION

Experimental investigations performed at ASDEX Upgrade showed that pellet pacing can raise the ELM frequency and reduce the power load on the divertor per ELM. With the available injection system, almost a doubling of the ELM frequency and according mitigation has been demonstrated [1]. Hence, pellet pacing can be considered as a potential tool for solving problems expected for ITER type-I ELM standard scenarios. Under the expected plasma conditions, scaling predicted power flux densities during intrinsic ELMs may be several times above the threshold required for a safe and enduring divertor operation. To be reliable scalings have to contain mid-size and larger tokamaks to ensure proper extrapolation to ITER dimensions. Based on the established stepladder concept of AUG-JET-ITER, the ITER size can be approched by investigating pellet ELM triggering at JET.

2. EXPERIMENTAL SET UP AND ANALYSIS STRATEGY

As the JET pellet system is not operational at the moment, the analysis was performed on former pellet injection experiments dedicated to particle fuelling. Although the pellet size (4mm cubes, nominal 3.8×10^{21} D) was far from ideal for ELM pacing conditions and the 6Hz repetition rate is significantly lower than the intrinsic ELM frequency, the experiments were found useful to study the ELM onset triggered during pellet ablation. Pellets were injected by varying their speed on a shot-to-shot basis in the range of 150 to 300m/s penetrating about to $\rho = 0.7-0.8$ enhancing the plasma particle inventory by about 10–30%. Launching was performed along the three designated injection trajectories referred to as H, V and L as shown in figure 1 with switching between tracks during a discharge. In addition to the poloidal cross-section of JET at octant 2, figure 1 displays the pellet monitor and the area covered by the vertical Soft X-Ray (SXR) cameras. D_α radiation from the ablation zone can be used to measure the ablation rate but D_α radiation from regions close to the first wall may result in additional traits in the pellet monitor signal. The pellet observation view covers the initial part of the H track in the plasma but misses the ablation onset for V and L pellets, the latter due to a slight toroidal displacement. Onset of strong burst like MHD activity provides a reliable and fast onset marker of ELMs. Signals from Mirnov coils mounted at different toroidal and poloidal locations were employed for the detection.

The High Triangularity (HT) plasma con configuration chosen was driven well into the H-mode regime (threshold 8MW) by applying a total heating power of 18.5MW. Plasmas developed an ELM-free phase lasting for about 100ms followed by sequences of clear type-I ELMs at about 50Hz of similar duration. Initial ELMs displayed amplitudes 2–4 times higher than the remaining ELMs in the train. From an ELM pacing point of view the experimental conditions (at least for the first pellets in the train) were well suited to study ELM triggering expected at the onset of pellet ablation. Only data with sufficient temporal resolution were selected for this analysis, thus the database includes 5H (all 150m/s), 10V (7 at 150m/s, 3 at 240m/s) and 1 L (240m/s) tracked pellets.

3. RESULTS

3.1 RELIABLE ELM TRIGGERING BY PELLETS

Con Confirming and broadening earlier findings in hot-ion discharges [2], it was found that every investigated pellet (included additional 200 not part of the database) injected during a type-I or an ELM free phase released an ELM. Obviously, ELM onset can be triggered at any stage of the intrinsic type-I ELM cycle or anytime during ELM free phases. An example is shown in figure 2 displaying several intrinsic and two triggered ELMs. One is triggered within an ELM train shortly after an intrinsic event, the other terminating an ELM-free phase. Besides the fact that fuelling size pellets trigger ELMs at a time intrinsic ones are unlikely to appear they also transiently alter the ELM behaviour. Due to strong fuelling resulting in a massive out flux of particles, the triggered ELM is followed by an ELM cascade of events intensified in comparison to intrinsic ones.

3.2 PROMPT ELM TRIGGERING BY PELLETS

Both triggered ELMs displayed in figure 2 show indications that they consist of two components. The first is hefty and short, the second gradual and persistent. The first component is the desired promptly triggered ELM induced by the local pellet perturbation in the edge region, as will be shown in the following. The second can be a strong limitation for the pellet pacing approach and should therefore be avoided or at least minimized by choosing pellet parameters restricting unwanted fuelling to the lowest possible amount. The decisive questions and hence subject of our detailed investigation is: when and where does the pellet trigger this prompt ELM and consequently what would be the minimum required size for pacing pellets. It is ultimately this value that determines the usefulness of the pellet pacing tool. Pellet ablation and resulting ELM behaviour was investigated for all three di different injection locations. For every one of them the first strong ELM component clearly starts early in the ablation process when only a small portion of the pellet mass has been ablated. However, the precise start of the ablation onset in the vicinity of the separatrix granted by direct observation is only recorded for the H track.

Hence, determination of the prompt ELM onset and estimation of the minimum pellet mass ablation at that time can only be performed for this case. An example is given in figure 3 displaying a pellet triggered and, for comparison, an intrinsic ELM. This comparison unveils the similarity of ELM fingerprints in the monitor signal for an intrinsic and a promptly triggered ELM. The ablation monitor signal recorded for the intrinsic ELM reveals there is radiation arising from the ELM. This additional component is superposed on the gradually increasing ablation radiation signal, causing an additional hump on it. The kink in the ablation monitor signal resulting from the sharp onset of this hump also correlates with the ELM onset in the MHD monitor signal and is therefore taken as the ELM onset. By eliminating the direct ELM radiation and assuming the remaining D_α radiation is proportional to the ablation rate, it was calculated that the pellet only loses about 1% of its initial mass by the time of the ELM onset.

By attributing the ablation onset to be the pellet crossing the separatrix, a penetration depth Δs of about 30mm along the designated path is obtained for the pellet shown in figure 2. With the H track tilted by 40 degrees with respect to the horizontal, the pellet radially only penetrates Δr = 20mm inside the separatrix. For all H track pellets in the database, an ELM onset delay of 200±30μs is derived, leading to Δs = 30±4.5mm or Δr = 23±3.4mm, respectively.

4. COMPARISON OF TRIGGER, ELM AND PELLET PERTURBATIONS

To release an ELM even a minor fraction of the fuelling sized pellet is sufficient. An illustration of the prompt ELM being triggered without significant changes of the local plasma density and temperature is presented in figure 4. It shows the evolution of the SXR emission profile, indicated by equal intensity contour lines, for an intrinsic (upper) and a pellet triggered ELM (lower). While the ELM evolves, the increasing energy out flux and particle recycling at the wall causes additional D_α radiation from the observation area, creating a small hump in the intrinsic reference and a larger additional hump in the triggered case. The higher D_α radiation is attributed to higher particle losses from the edge due to the increase of the local density beyond the equilibrium level as the pellet deposits its mass in this region.

The SXR emissivity change is attributed to the reduced local temperature caused by the pellet induced cooling effect, that can be observed when the triggered ELM and its resulting edge cooling sets in. The ELM then dominates the edge region for about 0.2ms before the pellet impact gradually becomes dominant again. In its final stages of ablation, the pellet's cooling e effect in the edge region exceed that of a typical ELM by a factor of 10, and it exceeds that imposed by the pellet at the moment when it triggers an ELM by about a factor of 100. Once more it seems clear that the pellet impact required for ELM pacing is small compared to the ELM impact itself, however the fuelling sized pellets potentially spoils any advantage of pacing by the large perturbation it causes.

CONCLUSIONS

Pellet injection was found to be a suitable tool to trigger ELMs in type-I ELMy and ELM-free phases of the JET tokamak. Detailed investigations of the triggered ELM onset dynamics in comparison with the ablation evolution demonstrated prompt triggering relying on a sufficiently strong local perturbation in the edge - shown before only in mid-size experiments - indeed works on a JET-size machine. Therefore, the ELM pacing approach seems to have a promising perspective to be applied even at reactor scales. Pellets with a particle content of only about 4×10^{19}D could prove sufficient for ELM pacing in JET but will eventually require reduced radial velocities in order to compensate for the ablation rate reduction related to the pellet size. Hence, the resulting particle fluxes may possibly be suppressed to negligible amounts eliminating any fuelling constraint that currently hampers the investigations.

REFERENCES

[1]. Lang, P.T. et al., Nucl. Fusion **43** (2003) 1110.
[2]. Alper, B. et al., 29th EPS conference (2002) P1.025.

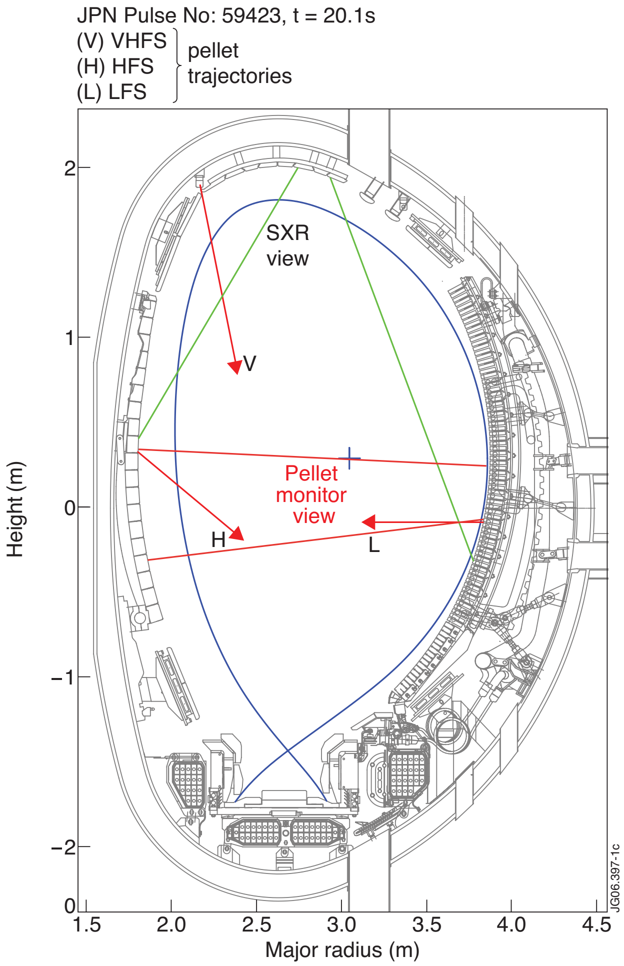

Figure 1: Poloidal cross section of JET octant 2 with a typically used plasma separatrix contour, the three designated pellet injection tracks, observation areas covered by SXR camera and pellet ablation monitor.

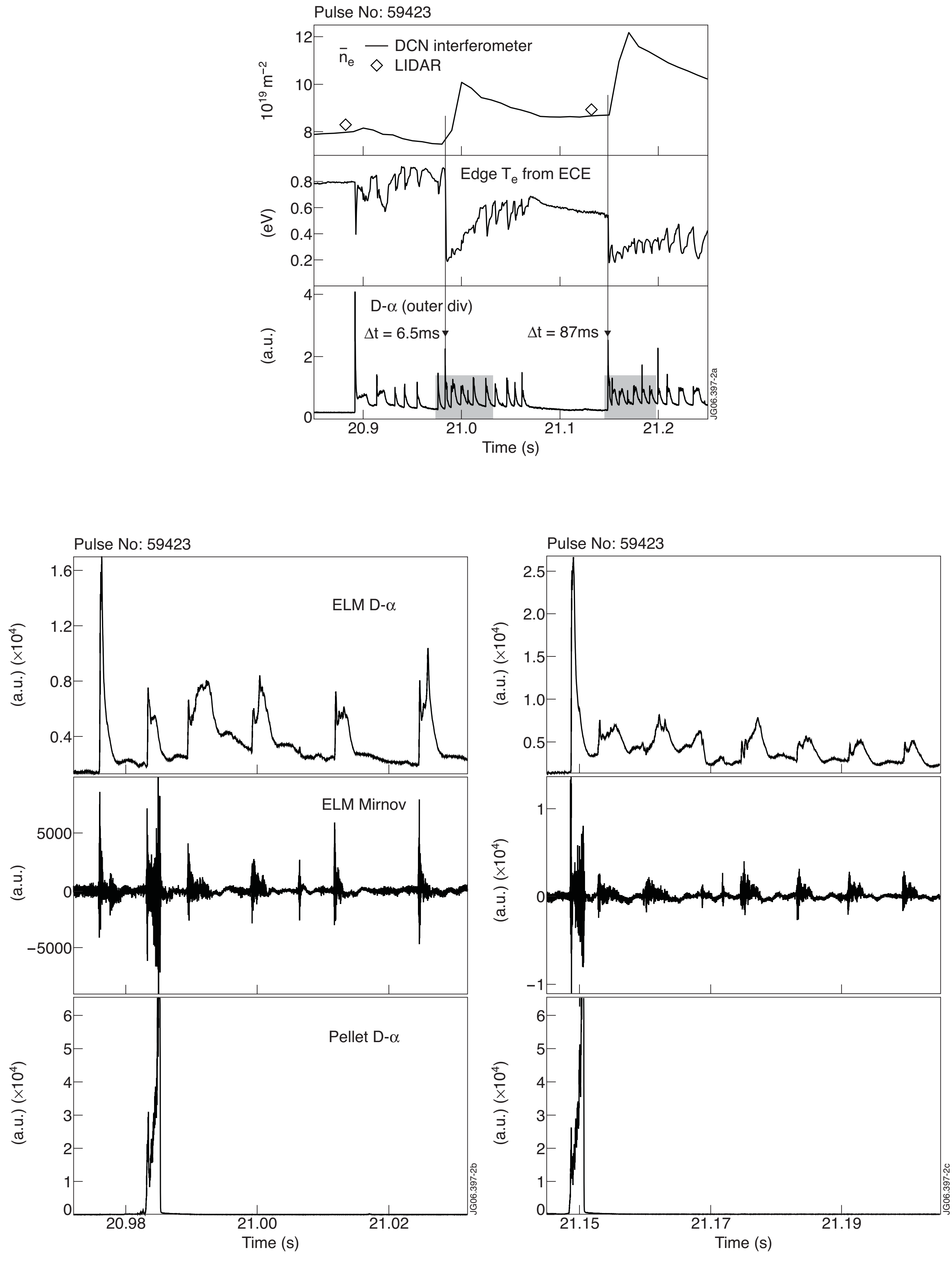

Figure 2: Pellets triggering ELMs at arbitrary times in the ELM cycle. Upper: Two pellets triggering ELMs despite different elapsed time since previous event. Hatched sequences displayed on expanded time scale below. Pellet induced ELMs consists of a fast and a slow component, the latter attributed to global fuelling.

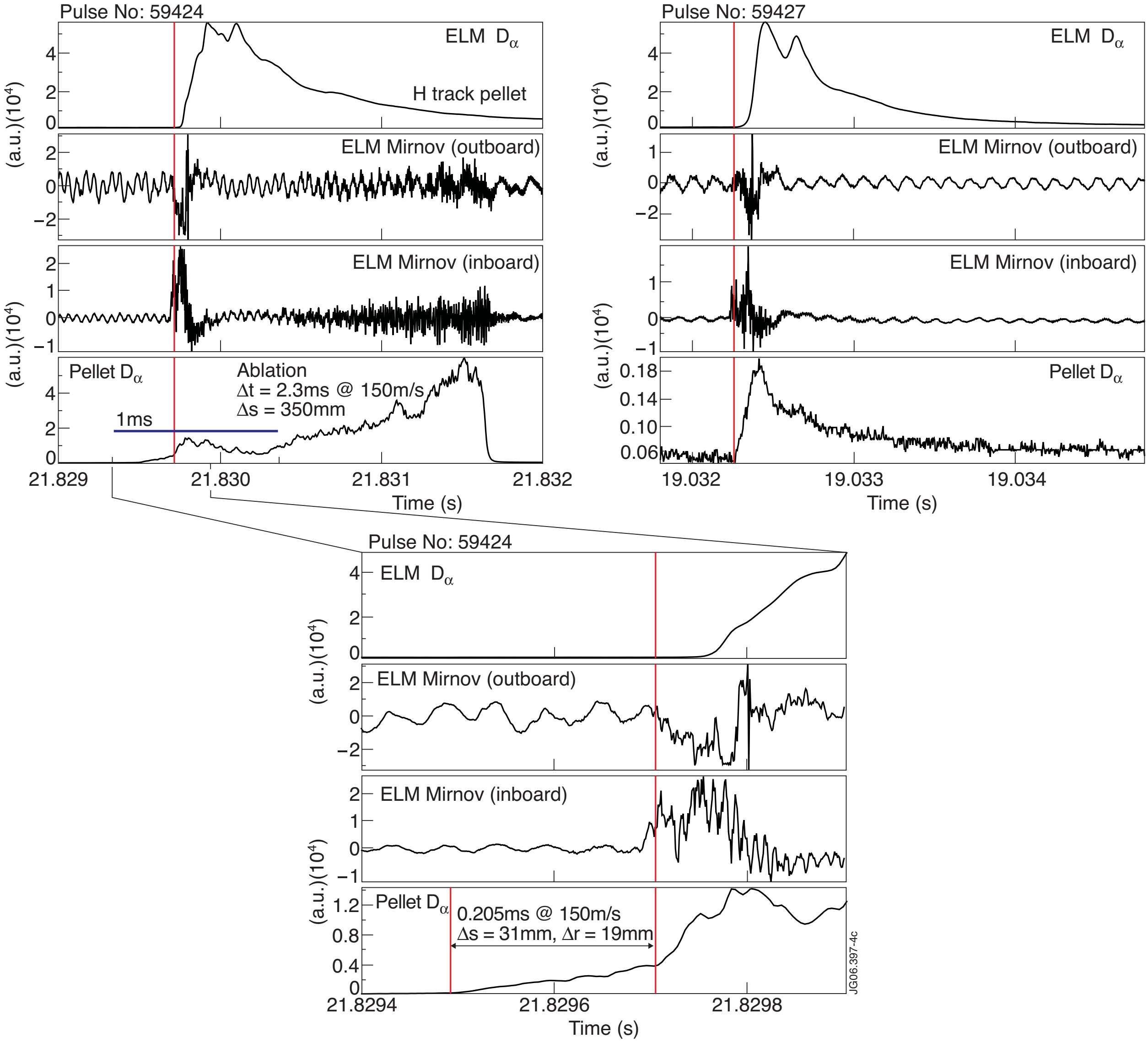

Figure 3: Upper: Comparison of triggered (left) and intrinsic (right) ELM. Signals from top: D outer divertor, MHD outboard and inboard ELM monitors, ablation monitor. Lower: expansion of ablation and ELM onset for triggered ELM.

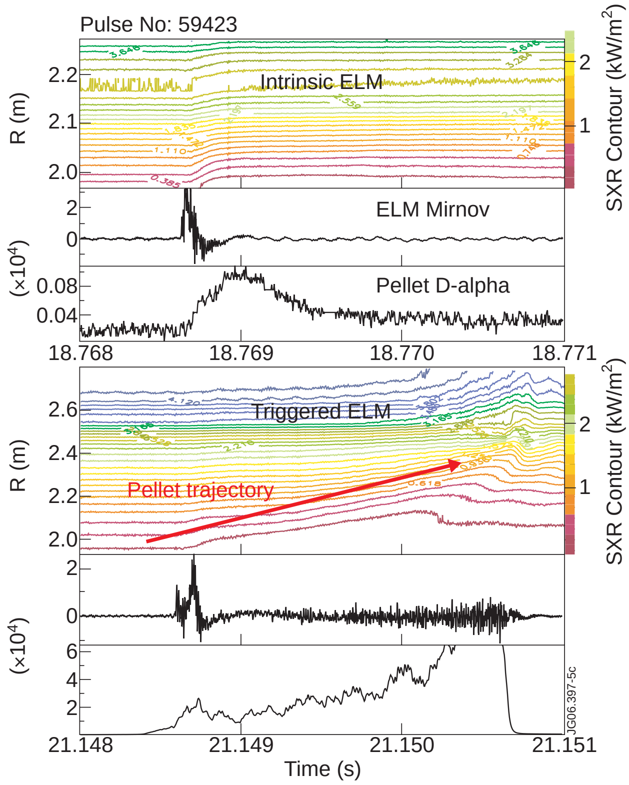

Figure 4: SXR evolution for intrinsic (upper) and pellet triggered ELM (lower). Pellet motion along designated trajectory mapped into the SXR pattern. ELM Mirnov monitor displays the ELM onset in the course of pellet ablation.